ACS Sustainable Chemistry & Engineering

Research Article

pubs.acs.org/journal/ascecg

Controlled Formation of Hierarchical Metal−Organic Frameworks Using CO_2-Expanded Solvent Systems

Huan V. Doan,[†,‡] Yanan Fang,[§] Bingqing Yao,[§] Zhili Dong,[§] Timothy J. White,[§] Asel Sartbaeva,[∥] Ulrich Hintermair,*[,⊥] and Valeska P. Ting*[,†]

[†]Department of Mechanical Engineering, University of Bristol, Bristol BS8 1TR, United Kingdom

[‡]Department of Oil Refining and Petrochemistry, Faculty of Oil and Gas, Hanoi University of Mining and Geology, Duc Thang, Bac Tu Liem, Hanoi, Vietnam

[§]School of Materials Science and Engineering, Nanyang Technological University, 11 Faculty Avenue, Singapore 639977

[∥]Department of Chemistry, University of Bath, Claverton Down, Bath BA2 7AY, United Kingdom

[⊥]Centre for Sustainable Chemical Technologies, University of Bath, Claverton Down, Bath BA2 7AY, United Kingdom

Supporting Information

ABSTRACT: It is shown that a crystalline metal−organic framework (HKUST-1) can be rapidly synthesized from a DMSO/MeOH solution with greatly reduced amounts of organic solvents using a supercritical CO_2 ($scCO_2$) solvent expansion technique. The precursor solution is stable for months under ambient conditions, and CO_2-driven MOF (metal−organic framework) crystallization is achieved under mild conditions (40 °C, 40−100 bar) with excellent reproducibility. As the degree of liquid-phase expansion drives MOF nucleation and growth, the crystallite size and overall yield can be tuned by adjusting the CO_2 pressure. Furthermore, scanning electron microscopy (SEM), high-resolution transmission electron microscopy (HR-TEM), and gas sorption analyses showed that, in the presence of $scCO_2$, HKUST-1 crystallites with a hierarchical pore structure are generated through a postcrystallization etching process. These findings demonstrate that $scCO_2$ is a time- and material-efficient route to MOF synthesis with a high level of control over the crystallization process for accessing tailored material properties.

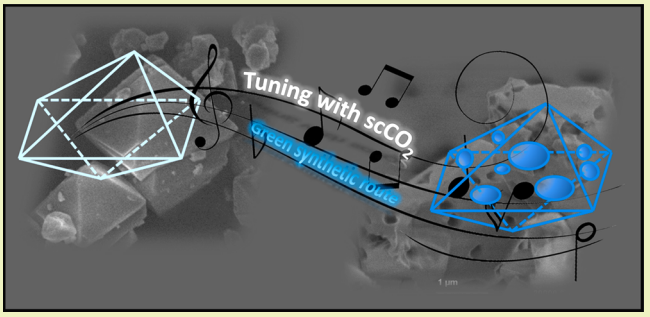

KEYWORDS: *Metal−organic frameworks, HKUST-1, Supercritical CO_2, Expanded liquid phases, Hierarchical porosity*

INTRODUCTION

Porous materials are attracting considerable attention for numerous applications because of their ability to interact with molecules, not only at their surfaces, but also within the internal cavities. An interesting class of materials which have a wide range of surface areas and porosities are the metal−organic frameworks (MOFs), which are extended coordination polymers built from metal ions/metal clusters and organic linkers. These architectures are of interest because of their permanent porosity and flexible linking of metal-cluster nodes and organic ligands, leading to high porosity, chemical stability, and thermal resistance.[1,2] The metal-containing units in MOFs, also called secondary building units (SBUs), are rigid squares, tetrahedra, or octahedra that self-assemble to form designed topologies, creating permanent porosity. The ability to systematically vary the size and nature of MOF tunnels and cavities makes them promising candidates for applications in gas separation and storage, and catalysis.[3−10]

One of the most stable nanoporous MOFs is copper trimesate (CuBTC) $\{Cu_3[(O_2C)_3C_6H_3]_2(H_2O)_3\}_n$ also known as HKUST-1 or MOF-199. This material, first reported in 1999 by Chui et al.,[11] has a cubic 3-D framework where the most abundant pore diameter is 11 Å. HKUST-1 can be synthesized by a solvothermal method in which $Cu(NO_3)_2$ and trimesic acid (benzene-1,3,5-tricarboxylic acid, BTC) are dissolved in DMF with a molar ratio Cu/BTC/DMF of 1:1:90,[12] whereupon nucleation proceeds rapidly after 30 min with the formation of a light-blue solid. This is exceptional for solvothermal MOF synthesis, which normally requires reaction times of several hours to days. Under basic conditions, precipitation occurred during precursor solution mixing; however, the solids formed were ill-defined and amorphous and showed neither the morphology nor the composition of the desired MOF.[13,14] Subsequently, a refined method using DMSO instead of DMF or DEF without additional base prevented premature precipitation, resulting in a very stable HKUST-1 precursor solution even at concentrations as high as 0.5 mol L^{-1}.[15] Addition of a several-fold excess of methanol

Received: May 7, 2017
Revised: July 26, 2017
Published: July 27, 2017

DOI: 10.1021/acssuschemeng.7b01429
ACS Sustainable Chem. Eng. 2017, 5, 7887−7893

Scheme 1. HKUST-1 Crystallization Reaction

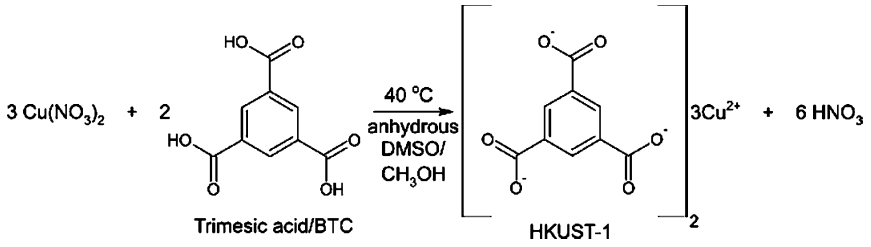

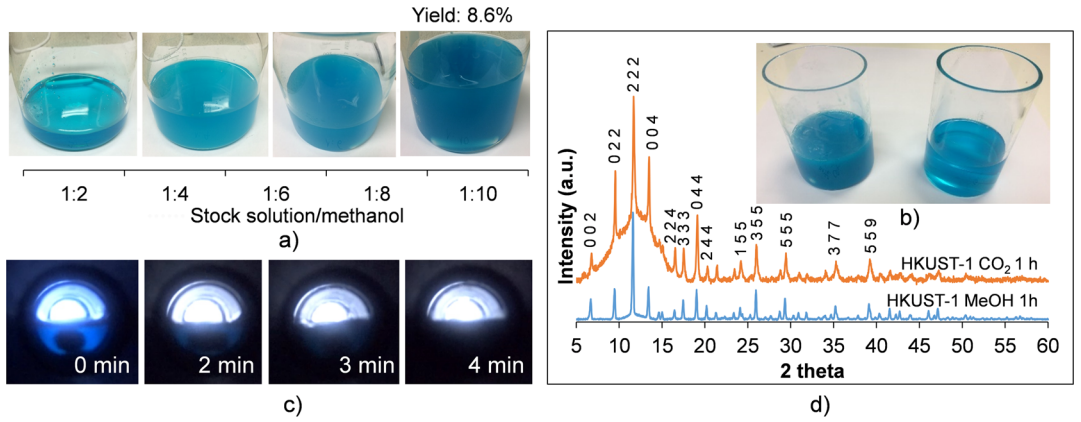

Figure 1. HKUST-1 formation driven by solvent expansion with CO_2. (a) Conventional HKUST-1 synthesis with different ratios of DMSO to methanol. (b) Precursor solution as 1:1 mixture of DMSO/MeOH after 72 h at 40 °C in air (right) and after exposure to 75 bar CO_2 (left). (c) Observation of HKUST-1 synthesized with 65 bar CO_2 in a view cell. (d) PXRD diffraction peaks of HKUST-1 synthesized by the conventional MeOH excess method compared to using CO_2-induced solvent expansion.

then triggered MOF crystallization within 10 min at room temperature, yielding 2 μm octahedral HKUST-1 crystals of uniform size.[16]

While appropriate on a laboratory scale, the use of large amounts of organic solvents, many of which are volatile, harmful, and flammable, is detrimental to the environment and expensive at a large scale. Therefore, alternative methods for synthesizing porous MOFs have been investigated, mainly focused on nonconventional solvents including supercritical fluids (SCFs),[17,18] ionic liquids,[19] and fluorinated solvents.[20] More recently, "zero-solvent" approaches using solid-phase[21] and gas-phase[22] syntheses have been developed. Although requiring high pressure, SCFs reduce not only the quantities of solvents needed, but also the energy and time required for separation of the SCF from the porous product, because the traditional multiple exchange, filtration, and drying steps are unnecessary.[23] In addition, because of their low surface tension and capillary forces, removal of the SCF solvent minimizes pore collapse during purification, which can be significant for highly porous materials.[24] This feature has long been exploited for the fabrication of aerogels[25] and, more recently, ultra-high-surface-area MOFs,[26] but somewhat surprisingly, SCF MOF synthesis and purification have rarely been combined so far.

In a separate line of research, the development of tailor-made porous materials exhibiting so-called hierarchical pore structures has attracted considerable current interest.[27,28] These intriguing materials combine micro-, meso-, and macroporosity within one structure, which not only enhances the total surface area, but also facilitates diffusional processes within the solid, thereby improving catalytic activity.[29]

Inspired by recent work, where HKUST-1 synthesized from $Cu(OAc)_2$ with BTC and NEt_3 in DMF diluted with liquid CO_2 showed modified pore sizes,[23] this study sought to investigate how MOF crystallization may be controlled by CO_2-induced solvent expansion. Specifically, the influence of the mixed media on the product structure was examined. For an assessment of the intrinsic porosity, the materials were subjected to postsynthetic continuous-flow $scCO_2$ (supercritical CO_2) extraction.

EXPERIMENTAL METHODS

All chemicals were sourced from commercial suppliers and used without further purification (Table S1 in the Supporting Information). The general synthesis procedure of HKUST-1 is summarized in Figure S1. Conventional HKUST-1 was prepared following Ameloot et al.[15] with a 20-fold scale-up. First, a stock solution was made by dissolving 24.52 g of copper(II) nitrate hemipentahydrate ($Cu(NO_3)_2 \times 2.5 H_2O$) (10.54 mmol) and 11.66 g of benzene-1,3,5-tricarboxylic acid (trimesic acid/BTC) (5.54 mmol) in 100 mL of dry DMSO. This deep-blue solution was stable over at least 6 weeks at ambient conditions (Figure S2a,b). To induce HKUST-1 formation, 10 mL of the stock solution was magnetically stirred at 200 rpm in a glass beaker, and 100 mL of methanol was added in one portion; the sample was heated to 40 °C for 1 h with continuous stirring. The HKUST-1 crystallization reaction is shown in Scheme 1. Product formation was made evident by the formation of a pale turquoise precipitate within 10 min. The product was isolated by centrifugation (3000 rpm for 20 min), washed with pure methanol, and recentrifuged three times. The clear, colorless solvent was finally decanted and the product dried in air at room temperature to yield 436 mg of a deep-blue microcrystalline powder (8.6 wt % yield).

For experiments using CO_2 instead of methanol, 40 mL of the stock solution was added to a glass vial containing 40 mL of methanol, which did not lead to a color change or precipitation. The vial was placed inside a stainless-steel high-pressure vessel (V = 250 mL), stirred with a magnetic bar at 200 rpm, heated to 40 °C, and pressurized with CO_2 at a flow rate of 5 g min^{-1}. The vessel was then sealed and left stirring

DOI: 10.1021/acssuschemeng.7b01429
ACS Sustainable Chem. Eng. 2017, 5, 7887−7893

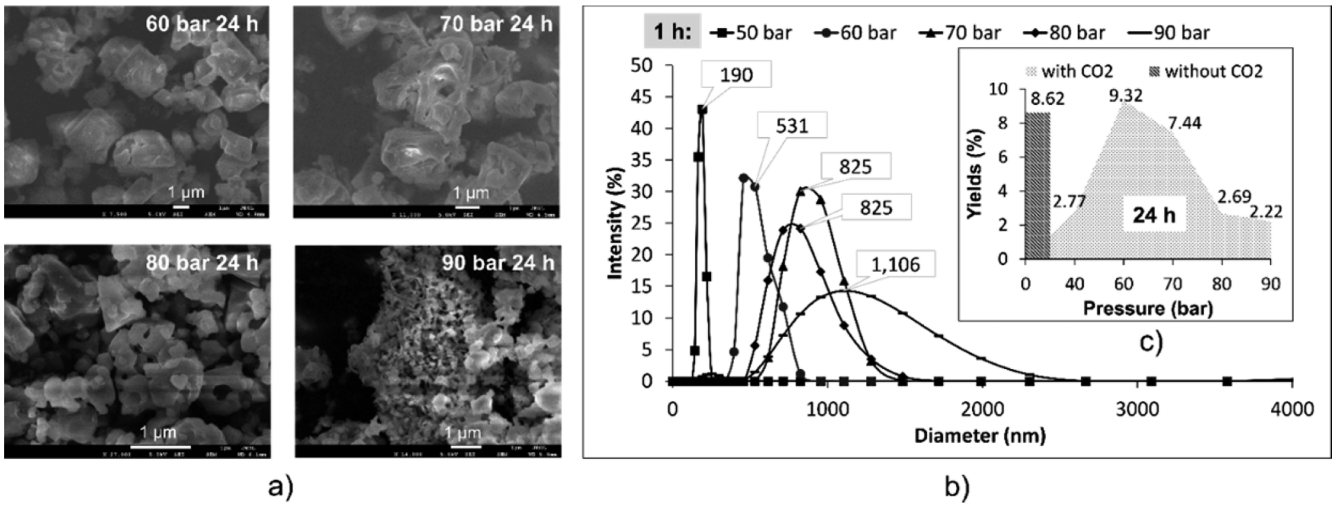

Figure 2. Effect of CO_2 pressure on HKUST-1 particle sizes and yields obtained from 1:1 DMSO/MeOH solution at 40 °C. (a) SEM images of HKUST-1 synthesized with different CO_2 pressures after 24 h. (b) Particle size distribution of HKUST-1 synthesized with different CO_2 pressures after 1 h. (c) Yields of HKUST-1 formation synthesized with different CO_2 pressures after 24 h.

Table 1. BET Surface Areas and Total Pore Volumes of HKUST-1 Samples Precipitated with Different Antisolvents at Varying Reaction Times[a]

	MeOH 1 h	70 bar CO_2 1 h	70 bar CO_2 24 h	70 bar CO_2 48 h	70 bar CO_2 72 h
surface area (m^2 g^{-1})	2032 ± 2	1616 ± 3	1693 ± 2	1409 ± 2	1220 ± 1
t-plot micropore area (m^2 g^{-1})	1698	1446	1197	1224	1094
total pore volume (cm^3 g^{-1})	0.811	0.592	0.794	0.666	0.545
t-plot micropore volume (cm^3 g^{-1})	0.667	0.557	0.591	0.474	0.420

[a]All at 40°C, all $scCO_2$ extracted prior to analysis.

at 40 °C. Reaction times ranged from 1 to 72 h and pressures between 40 and 90 bar (Table S2). High-pressure view-cell experiments were carried out in a 20 mL stainless-steel vessel with opposing windows of single crystal sapphire using 1.5 mL of DMSO stock solution combined with 1.5 mL of methanol under otherwise identical conditions.

All products were dried further by continuous-flow $scCO_2$ extraction. A sample of 0.1−0.3 g of solid was placed in 2 cm dialysis tubing (cellulose, 1000 MW cutoff), sealed with copper wire (see Figure S2d), and then placed into stainless-steel high-pressure tubing (0.5 in. diameter, 10 cm length) with a 50 μm particulate filter at the outlet. The sample was subjected to continuous $scCO_2$ extraction at 40 °C and 120 bar (d = 0.69 g/mL) with 2 g CO_2 min^{-1} over 18 h using a custom-built SCF continuous-flow rig similar to that previously described.[30] The plug-flow reactor was then depressurized at 10 bar min^{-1}, and the sample was recovered and analyzed immediately. After drying, the sample color had changed from dark to light blue (Figure S2f,g) with a weight loss of 6−10% due to extraction of the residual moisture and solvent.[31,32]

For an investigation of the potential solubility and postsynthetic modification of crystalline HKUST-1 in methanol and DMSO, 0.1 g of conventionally synthesized HKUST-1 was added to a mixture of 40 mL of methanol and 40 mL of DMSO, and stirred magnetically at 200 rpm and 40 °C for 48 h (Figure S2c), after which time the material was recovered unchanged.

The porous MOFs were characterized by powder X-ray diffraction (PXRD), gas sorption analysis, scanning electron microscopy (SEM), high-resolution transmission electron microscopy (HR-TEM), and dynamic light scattering (DLS). Details of these experiments are provided in the Supporting Information.

RESULTS

Using CO_2 as Antisolvent for HKUST-1 Synthesis. As reported previously, HKUST-1 nucleation from DMSO can be promoted by either evaporating at 373 K over 24 h or by adding methanol as an antisolvent to prompt nucleation. The latter method requiring 50 times excess methanol[16] is challenging in large-scale batch-wise synthesis; thus we investigated the amount of required antisolvent by systematically varying the ratio of methanol to DMSO stock solution (1:1, 2:1, 4:1, 6:1, 8:1, and 10:1 by volume) while monitoring HKUST-1 formation (Figure 1a). It was found that a 4-fold excess of methanol is the minimum to induce nucleation within 1 h, with higher yields obtained with more MeOH. In common with the pure DMSO precursor solution, 1:1 mixtures of DMSO and MeOH failed to produce any solid even after 6

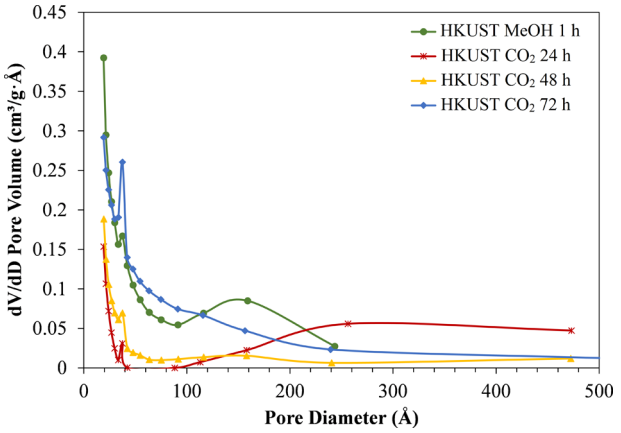

Figure 3. Mesopore size distribution curves for HKUST-1 samples precipitated with different antisolvents at varying reaction times (all at 40 °C, all $scCO_2$ extracted prior to analysis).

DOI: 10.1021/acssuschemeng.7b01429
ACS Sustainable Chem. Eng. 2017, 5, 7887−7893

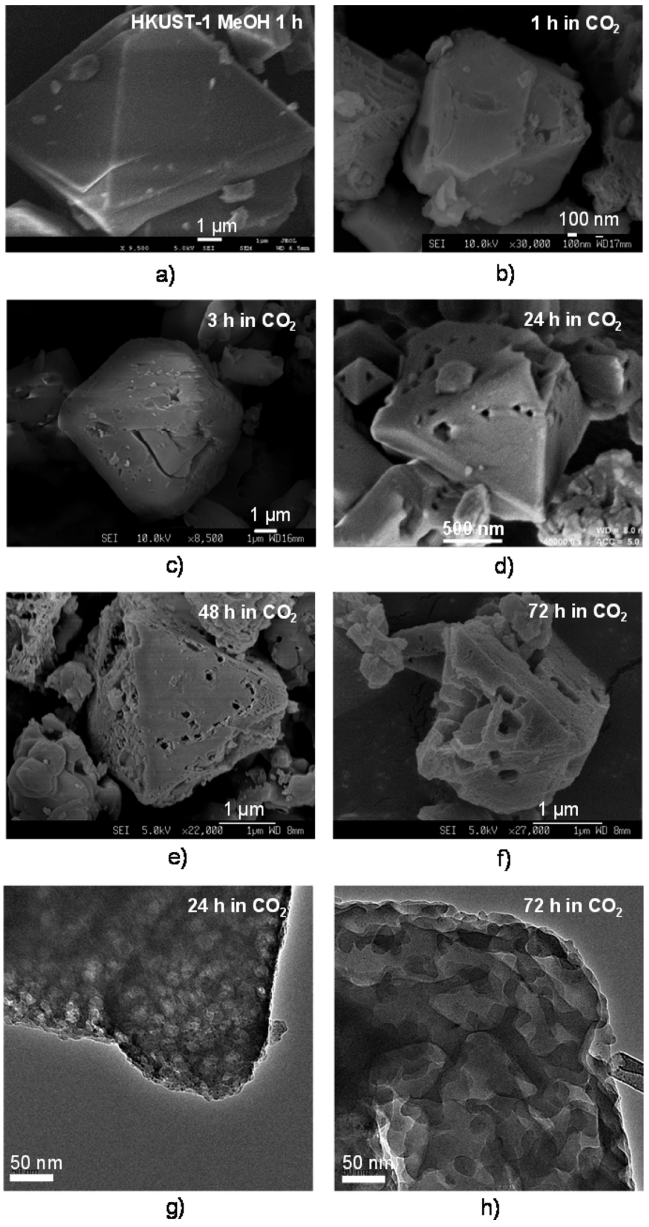

Figure 4. SEM and HR-TEM images of HKUST-1 synthesized using different antisolvents and reaction times (all at 40 °C). (a) HKUST-1 crystallized from DMSO with excess MeOH (1 h). (b–f) HKUST-1 crystallized from 1:1 DMSO/MeOH with 75 bar CO_2 (1, 3, 24, 48, and 72 h, respectively). (g,h) HR-TEM of HKUST-1 crystallized from 1:1 DMSO/MeOH with 75 bar CO_2 (24 and 72 h, respectively).

weeks at room temperature. Thus, the possibility of inducing HKUST-1 formation from neat DMSO and 1:1 DMSO/MeOH solutions by expansion with CO_2 was investigated. Many liquid organic compounds (including DMSO and MeOH) form so-called type-II solvent mixtures of high mutual solubility with compressed CO_2 in the near-critical region (i.e., around p_c, but above T_c).[33] The dissolution of large amounts of CO_2 leads to volumetric expansion of the solvent (up to 10 times the initial volume), and these expanded liquid phases (ELPs) show a range of interesting (tunable) physicochemical properties.[34] In the case of DMSO, the decrease in polarity and disruption of the stabilizing hydrogen-bonding interactions that prevent premature HKUST-1 formation[35,36] in the absence of an antisolvent were expected to be the trigger for CO_2-induced MOF crystallization.

It was found that HKUST-1 formation could not be induced by expanding pure DMSO precursor solutions with 90 bar CO_2 for 72 h at 40 °C. However, pressurizing the equally stable 1:1 DMSO/MeOH mixture with CO_2 at 40 °C resulted in a blue precipitate in yields of 4–9% (depending on conditions; see below) that did not redissolve upon depressurization. PXRD showed the solid to be pure HKUST-1 (Figure 1d), and SEM revealed octahedral crystallites ~2 μm in size, similar to conventional synthesis using >10-fold excess of MeOH (Figure 4a). This confirms that MOFs can be synthesized by CO_2-induced solvent expansion using greatly reduced amounts of organic solvent. As the solubilities of CO_2 in DMSO and MeOH are very similar,[37] leading to a similar volume expansion[37] and a concomitant decrease in polarity[38] with the addition of CO_2, it is concluded that H-bonding disruption must be the effective driving force for CO_2-induced HKUST-1 crystallization from DMSO/MeOH mixtures.

When the reaction was followed in a high-pressure view cell at 40 °C, a precipitate was observed within 2 min after introducing 65 bar of CO_2 to the reactor, and a fully opaque mixture was obtained after 4 min (Figure 1c). Thus, CO_2-driven HKUST-1 crystallization from the DMSO solution is faster than that with excess MeOH, yet produces a phase-pure crystalline material unlike when using DMF and/or additional bases.

Effect of CO_2 Pressure on HKUST-1 Yields and Particle Sizes. For an investigation of how the CO_2 content in the expanded liquid phase affects HKUST-1 formation, the applied CO_2 pressure was varied from 40 to 90 bar while temperature, reaction time, and flow rate were held constant (40 °C, 24 h, and 5 g min^{-1}). Longer reaction times were chosen for these experiments to ensure that equilibrium was established. Figure 2c shows that up to 60 bar CO_2 the yield of HKUST-1 increased to levels obtained with an excess of organic antisolvent. At higher pressures the yields decreased again, an observation ascribed to a decrease in pH with increasing pressure, which progressively destabilizes the product. This is supported by the known sensitivity of HKUST-1 to acidic media[27,28] and our observation of postsynthetic etching effects described below.

SEM showed that, up to 70 bar CO_2, the particle sizes obtained were comparable to those of the conventionally synthesized material, but at higher pressures, smaller particles with ill-defined shapes formed, despite retaining their crystallinity (Figure 2a). Lowering the pressurization rate from 5 to 0.1 g min^{-1} for 75 bar CO_2 gave similar yields and crystallite sizes (Table S2), indicating that the amount of CO_2 added is the dominant factor in the crystallization process, rather than its rate of addition.

To gain a deeper insight into how CO_2 pressure affects crystallite nucleation and growth, particle size distributions were analyzed by dynamic light scattering (DLS) after 1 h reaction time (Figure 2b). Under these conditions, applying 40 bar of CO_2 produced insignificant amounts of HKUST-1. However, at 50 bar and above, the DLS results showed a direct relationship between pressure and average particle size, with dispersity increasing substantially at a higher pressure. This behavior suggests more rapid nucleation at higher pressures, likely due to the larger amounts of antisolvent added. These results demonstrate that particle sizes and dispersity can easily be controlled over a wide range simply by varying the CO_2

DOI: 10.1021/acssuschemeng.7b01429
ACS Sustainable Chem. Eng. 2017, 5, 7887–7893

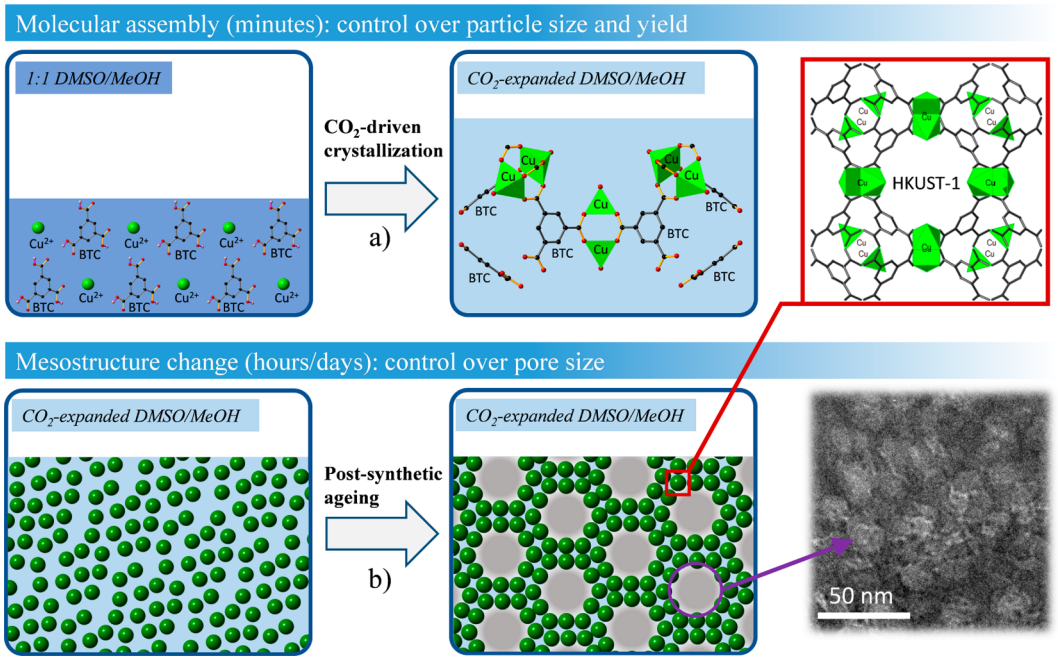

Figure 5. Schematic illustration for HKUST-1 crystallization (a) and meso/macropore formation (b) in the CO_2-expanded solvent.

pressure applied (if the temperature is kept above T_c to avoid condensation).

Effect of CO_2 Exposure on HKUST-1 Porosity. For confirmation of the production of porous HKUST-1 crystallites and an assessment of the influence of CO_2 on their pore structure, nitrogen adsorption/desorption analysis at 77 K was performed following $scCO_2$ extraction of the isolated materials. The samples synthesized by CO_2-induced solvent expansion showed the typical microporous isotherms expected of HKUST-1, with total pore volumes >0.5 $cm^3\ g^{-1}$ and BET surface areas >1000 $m^2\ g^{-1}$ (Figure S4). Interestingly, upon comparison of different reaction times under otherwise identical conditions, a small but consistent decrease in both surface areas and pore volumes the longer the samples had been left in the CO_2-expanded DMSO/MeOH solvent mixture is seen (Table 1). Analysis of the N_2 adsorption/desorption isotherms shows that this originates from a greater proportion of macropores which contribute less to surface area than micropores (Figure S4), which can also be seen in the SEM and TEM analyses. Figure 4b–f shows the change in morphology over time, with faceted macroporous crystallites and mesopores appearing in the samples left for 24 h (Figure 4d and Figure S5a). The number of mesopores increased with longer exposure to CO_2; after 72 h the microstructure consisted of a finely divided network of macro- and mesopores (Figure 4f and Figure S7a). For 24 and 72 h, the nature of the porosity was further confirmed by HRTEM (Figure 4j,k, Figures S5b and S7b). All samples produced PXRD patterns characteristic of HKUST-1 (Figure S3), confirming that the MOF framework was preserved.

Analysis of the differential pores size distributions (Figure 3) revealed that all samples precipitated from base-free 1:1 DMSO/MeOH solution, either with a 10-fold excess of MeOH or with 70 bar CO_2, showed the characteristically high, intrinsic microporosity of HKUST-1. Samples synthesized via CO_2 expansion of the DMSO/MeOH precursor solution showed added mesoporosity by N_2 adsorption analysis (Figure 3), though macropores, which contribute much less to pore volume and surface area than micro- and mesopores, were also clearly visible in the SEM images (Figure 4). These results differ from Peng's data[23] that showed almost exclusive mesoporosity for HKUST-1 synthesized from DMF/NEt_3 precursor solutions which in the absence of CO_2 form amorphous, nonporous solids.

In line with the observation of lower HKUST-1 yields at higher CO_2 pressures discussed above (Figure 2), we conclude that the additional acidity introduced by CO_2 induces postsynthetic aging in the CO_2-expanded DMSO/MeOH mixtures, leading to increased levels of meso- and macroporosity in the MOF crystallites. This observation, which to the best of our knowledge has not been previously described for an MOF,[39] represents another experimental variable of the CO_2 expansion method for MOF crystallization that allows fine-tuning of the properties of the resulting material. The possibility of adding larger pores and channels to a crystalline MOF without compromising its intrinsic highly microporous structure offers exciting prospects for applications in any process that may be limited by diffusional resistance to the internal surface. Importantly, crystallite size and porosity may be adjusted independently by the appropriate choice of CO_2 pressure and reaction time, respectively (Figure 5), allowing high levels of process control that may be challenging using conventional protocols. We anticipate that these principles may be applicable to many other MOFs that assemble from solution by way of antisolvent-driven crystallization, and are currently exploring the scope of this technique more widely.

CONCLUSION

It is demonstrated that crystalline, porous HKUST-1 can be synthesized using CO_2-induced solvent expansion as an alternative to adding copious amounts of organic solvents. HKUST-1 crystallization is triggered by the application of CO_2 to a stable 1:1 DMSO/MeOH precursor solution that does not form any precipitate in the absence of CO_2. Rapid nucleation and HKUST-1 crystallization occurs under 50–90 bar CO_2 at 40 °C to achieve yields comparable to those of conventional

DOI: 10.1021/acssuschemeng.7b01429
ACS Sustainable Chem. Eng. 2017, 5, 7887–7893

antisolvent methods. Considering that the CO_2 used for driving and controlling MOF crystallization can easily be recovered and reused, this method reduces the *E*-factor of the process by a factor of 4 from $E > 2000$ for the conventional method using excess MeOH[15] to $E \sim 500$ for the CO_2 expansion method, which may find wider use and lead to greener MOF production at a reduced environmental impact. Significantly, the CO_2 expansion technique allows tight control over crystallite size by adjustment of CO_2 pressure, and postsynthetic aging accelerated by the presence of CO_2 to create additional porosity. As this added meso- and macroporosity is interconnected with the intrinsic microporosity of the MOF, a truly hierarchical pore architecture is obtained that could prove beneficial for applications in gas separation and catalysis.

■ ASSOCIATED CONTENT

Supporting Information

The Supporting Information is available free of charge on the ACS Publications website at DOI: 10.1021/acssuschemeng.7b01429.

Additional experimental and analytical details including photographs of materials, powder XRD data, N_2 adsorption isotherms, and SEM and TEM images (PDF)

■ AUTHOR INFORMATION

Corresponding Authors

*E-mail: u.hintermair@bath.ac.uk.
*E-mail: v.ting@bristol.ac.uk.

ORCID

Huan V. Doan: 0000-0002-8757-364X
Zhili Dong: 0000-0001-8116-6747
Timothy J. White: 0000-0002-4380-9403
Ulrich Hintermair: 0000-0001-6213-378X
Valeska P. Ting: 0000-0003-3049-0939

Notes

The authors declare no competing financial interest.

■ ACKNOWLEDGMENTS

This research was supported by funding from the Vietnamese Government and the University of Bristol (studentship to H.V.D.), the University of Bath (International Mobility Funding with Nanyang Technological University), the Centre for Sustainable Chemical Technologies at the University of Bath (Whorrod Research Fellowship to U.H.), the Royal Society (University Research Fellowship to A.S.), and Nanyang Technological University (AcRF Tier1 funding to Z.D. and B.Y.). We thank Sonia Raikova (University of Bath) for preliminary work leading to this project, Laura Rodriguez Arco (University of Bristol) for help with the DLS measurements, and Sean Davis (University of Bristol) for help with the SEM experiments. We also thank the Facility for Analysis, Characterization, Testing and Simulation (FACTS) at Nanyang Technological University for the electron microscopy experiments.

■ REFERENCES

(1) Furukawa, H.; Cordova, K. E.; O 'Keeffe, M.; Yaghi, O. M. The chemistry and applications of metal-organic frameworks. *Science* **2013**, *341* (6149), 1230444.

(2) Kaskel, S. *The Chemistry of Metal-Organic Frameworks: Synthesis, Characterization, and Applications*; Kaskel, S., Ed.; Wiley-VCH Verlag GmbH & Co. KGaA: Weinheim, Germany, 2016.

(3) Zhou, H.-C.; Long, J. R.; Yaghi, O. M. Introduction to Metal−Organic Frameworks. *Chem. Rev.* **2012**, *112* (2), 673−674.

(4) Sumida, K.; Rogow, D. L.; Mason, J. A.; McDonald, T. M.; Bloch, E. D.; Herm, Z. R.; Bae, T.-H.; Long, J. R. Carbon Dioxide Capture in Metal-Organic Frameworks. *Chem. Rev.* **2012**, *112* (2), 724−781.

(5) Suh, M. P.; Park, H. J.; Prasad, T. K.; Lim, D.-W. Hydrogen Storage in Metal−Organic Frameworks. *Chem. Rev.* **2012**, *112* (2), 782−835.

(6) Wu, H.; Gong, Q.; Olson, D. H.; Li, J. Commensurate Adsorption of Hydrocarbons and Alcohols in Microporous Metal Organic Frameworks. *Chem. Rev.* **2012**, *112* (2), 836−868.

(7) Li, J.-R.; Sculley, J.; Zhou, H.-C. Metal−Organic Frameworks for Separations. *Chem. Rev.* **2012**, *112* (2), 869−932.

(8) Bétard, A.; Fischer, R. A. Metal−Organic Framework Thin Films: From Fundamentals to Applications. *Chem. Rev.* **2012**, *112* (2), 1055−1083.

(9) Yoon, M.; Srirambalaji, R.; Kim, K. Homochiral Metal−Organic Frameworks for Asymmetric Heterogeneous Catalysis. *Chem. Rev.* **2012**, *112* (2), 1196−1231.

(10) Horcajada, P.; Gref, R.; Baati, T.; Allan, P. K.; Maurin, G.; Couvreur, P.; Férey, G.; Morris, R. E.; Serre, C. Metal−Organic Frameworks in Biomedicine. *Chem. Rev.* **2012**, *112* (2), 1232−1268.

(11) Chui, S. S.-Y.; Lo, S. M.-F.; Charmant, J. P. H.; Orpen, A. G.; Williams, I. D. A Chemically Functionalizable Nanoporous Material [Cu3(TMA)2(H2O)3]n. *Science* **1999**, *283* (5405), 1148−1150.

(12) Shöâeè, M.; Agger, J. R.; Anderson, M. W.; Attfield, M. P. Crystal form, defects and growth of the metal organic framework HKUST-1 revealed by atomic force microscopy. *CrystEngComm* **2008**, *10* (6), 646.

(13) Gascon, J.; Aguado, S.; Kapteijn, F. Manufacture of dense coatings of Cu3(BTC)2 (HKUST-1) on α-alumina. *Microporous Mesoporous Mater.* **2008**, *113* (1), 132−138.

(14) Hermes, S.; Schröder, F.; Chelmowski, R.; Wöll, C.; Fischer, R. A. Selective Nucleation and Growth of Metal−Organic Open Framework Thin Films on Patterned COOH/CF3-Terminated Self-Assembled Monolayers on Au(111). *J. Am. Chem. Soc.* **2005**, *127* (40), 13744−13745.

(15) Ameloot, R.; Gobechiya, E.; Uji-i, H.; Martens, J. A.; Hofkens, J.; Alaerts, L.; Sels, B. F.; De Vos, D. E. Direct patterning of oriented metal-organic framework crystals via control over crystallization kinetics in clear precursor solutions. *Adv. Mater.* **2010**, *22* (24), 2685−2688.

(16) Zhuang, J.-L.; Ceglarek, D.; Pethuraj, S.; Terfort, A. Rapid Room-Temperature Synthesis of Metal-Organic Framework HKUST-1 Crystals in Bulk and as Oriented and Patterned Thin Films. *Adv. Funct. Mater.* **2011**, *21* (8), 1442−1447.

(17) Darr, J. A.; Poliakoff, M. New Directions in Inorganic and Metal-Organic Coordination Chemistry in Supercritical Fluids. *Chem. Rev.* **1999**, *99* (2), 495−542.

(18) Eckert, C. A.; Knutson, B. L.; Debenedetti, P. G. Supercritical fluids as solvents for chemical and materials processing. *Nature* **1996**, *383* (6598), 313−318.

(19) Blanchard, L. A.; Hancu, D.; Beckman, E. J.; Brennecke, J. F. Green processing using ionic liquids and CO2. *Nature* **1999**, *399* (6731), 28−29.

(20) Zhao, Y.; Zhang, J.; Han, B.; Song, J.; Li, J.; Wang, Q. Metal-Organic Framework Nanospheres with Well-Ordered Mesopores Synthesized in an Ionic Liquid/CO2/Surfactant System. *Angew. Chem., Int. Ed.* **2011**, *50* (3), 636−639.

(21) Crawford, D.; Casaban, J.; Haydon, R.; Giri, N.; McNally, T.; James, S. L. Synthesis by extrusion: continuous, large-scale preparation of MOFs using little or no solvent. *Chem. Sci.* **2015**, *6* (3), 1645−1649.

(22) Lausund, K. B.; Nilsen, O. All-gas-phase synthesis of UiO-66 through modulated atomic layer deposition. *Nat. Commun.* **2016**, *7*, 13578.

DOI: 10.1021/acssuschemeng.7b01429
ACS Sustainable Chem. Eng. 2017, 5, 7887−7893

(23) Peng, L.; Zhang, J.; Xue, Z.; Han, B.; Sang, X.; Liu, C.; Yang, G. Highly mesoporous metal−organic framework assembled in a switchable solvent. *Nat. Commun.* **2014**, *5*, 933−969.
(24) Cooper, A. I. Porous materials and supercritical fluids. *Adv. Mater.* **2003**, *15* (13), 1049−1059.
(25) Aegerter, M. A.; Leventis, N.; Koebel, M. M. *Aerogels Handbook*; Springer: New York, 2011.
(26) Farha, O. K.; Eryazici, I.; Jeong, N. C.; Hauser, B. G.; Wilmer, C. E.; Sarjeant, A. A.; Snurr, R. Q.; Nguyen, S. T.; Yazaydın, A. Ö.; Hupp, J. T. Metal−Organic Framework Materials with Ultrahigh Surface Areas: Is the Sky the Limit? *J. Am. Chem. Soc.* **2012**, *134* (36), 15016−15021.
(27) Hartmann, M.; Schwieger, W. Hierarchically-structured porous materials: from basic understanding to applications. *Chem. Soc. Rev.* **2016**, *45* (12), 3311−3312.
(28) Su, B.-L.; Sanchez, C.; Yang, X.-Y. Insights into Hierarchically Structured Porous Materials: From Nanoscience to Catalysis, Separation, Optics, Energy, and Life Science. In *Hierarchically Structured Porous Materials*; Wiley-VCH Verlag GmbH & Co. KGaA: Weinheim, Germany, 2011; pp 1−27.
(29) Parlett, C. M. A.; Wilson, K.; Lee, A. F. Hierarchical porous materials: catalytic applications. *Chem. Soc. Rev.* **2013**, *42* (9), 3876−3893.
(30) Hintermair, U.; Roosen, C.; Kaever, M.; Kronenberg, H.; Thelen, R.; Aey, S.; Leitner, W.; Greiner, L. A Versatile Lab to Pilot Scale Continuous Reaction System for Supercritical Fluid Processing. *Org. Process Res. Dev.* **2011**, *15* (6), 1275−1280.
(31) DeCoste, J. B.; Peterson, G. W.; Schindler, B. J.; Killops, K. L.; Browe, M. A.; Mahle, J. J.; Zecchina, A.; Solari, P. L.; Kongshaug, K. O.; Bordiga, S.; et al. The effect of water adsorption on the structure of the carboxylate containing metal−organic frameworks Cu-BTC, Mg-MOF-74, and UiO-66. *J. Mater. Chem. A* **2013**, *1* (38), 11922.
(32) Peterson, G. W.; Britt, D. K.; Sun, D. T.; Mahle, J. J.; Browe, M.; Demasky, T.; Smith, S.; Jenkins, A.; Rossin, J. A. Multifunctional Purification and Sensing of Toxic Hydride Gases by CuBTC Metal−Organic Framework. *Ind. Eng. Chem. Res.* **2015**, *54* (14), 3626−3633.
(33) Jessop, P. G.; Subramaniam, B. Gas-Expanded Liquids. *Chem. Rev.* **2007**, *107* (6), 2666−2694.
(34) Hintermair, U.; Leitner, W.; Jessop, P. Expanded Liquid Phases in Catalysis: Gas-Expanded Liquids and Liquid-Supercritical Fluid Biphasic Systems. In *Handbook of Green Chemistry*; Wiley-VCH Verlag GmbH & Co. KGaA: Weinheim, Germany, 2010.
(35) Bernès, S.; Hernández, G.; Portillo, R.; Gutiérrez, R. Trimesic acid dimethyl sulfoxide solvate: space group revision. *Acta Crystallogr., Sect. E: Struct. Rep. Online* **2008**, *64* (7), o1366.
(36) Persson, I. Solvation and Complex Formation in Strongly Solvating Solvents. *Pure Appl. Chem.* **1986**, *58*, 8, 10.1351/pac198658081153.
(37) Kordikowski, A.; Schenk, A. P.; Van Nielen, R. M.; Peters, C. J. Volume expansions and vapor-liquid equilibria of binary mixtures of a variety of polar solvents and certain near-critical solvents. *J. Supercrit. Fluids* **1995**, *8* (3), 205−216.
(38) Abbott, A. P.; Hope, E. G.; Mistry, R.; Stuart, A. M. Probing the structure of gas expanded liquids using relative permittivity, density and polarity measurements. *Green Chem.* **2009**, *11* (10), 1530.
(39) A similar change of morphology over time (in the absence of CO_2) has very recently been observed for the Zn-based zeolitic imidazolate framework ZIF-8. López-Periago, A. M.; Portoles-Gil, N.; López-Domínguez, P.; Fraile, J.; Saurina, J.; Aliaga-Alcalde, N.; Tobias, G.; Ayllón, J. A.; Domingo, C. Metal−Organic Frameworks Precipitated by Reactive Crystallization in Supercritical CO2. *Cryst. Growth Des.* **2017**, *17*, 2864.

DOI: 10.1021/acssuschemeng.7b01429
ACS Sustainable Chem. Eng. 2017, 5, 7887−7893